Wearable Human Body Communication Channel Measurements in the Body Resonance Regime

Samyadip Sarkar, Qi Huang, Mayukh Nath, Shreyas Sen
School of Electrical and Computer Engineering, Purdue University, West Lafayette, IN, USA
{sarkar46, shreyas}@purdue.edu

***Abstract*— Over the last couple of decades, Human Body Communication (HBC) has emerged as a promising alternative to wireless communication for energy-efficient data transfer using miniaturized wearable devices, and its channel characterization in the Electro-Quasistatics (EQS) regime has been widely explored. Moreover, three regions in the HBC channel characteristic, namely EQS, Body Resonance (BR), and Device Resonance (DR), over a broad frequency range from 100 kHz to 1 GHz, have been conceptualized. The BR region, with high channel gain (CG) and bandwidth, can potentially inspire the design of more power-efficient HBC systems than the state-of-the-art. In this paper, the channel measurements focusing on the body resonance regime (30 MHz to 250 MHz measurement frequency range) and variability caused by the receiver (Rx) position change are studied through measurements with wearable devices. Results illustrate that the human body improves the CG by ∼45 dB compared with transmission through the air. The placement of the receiver near the shoulder causes severe attenuations in CG, and higher frequencies cause larger CG undulation. Moreover, with T-posture, the body resonance peak appears between 100 and 150 MHz, which helps to select an optimum frequency for the HBC system design, supporting high data rates and power efficiencies.**

***Keywords*— Body Resonance (BR) Regime, Human Body Communication (HBC), Wearable-to-Wearable Measurements.**

I. Introduction

Over the last six decades, technology scaling has resulted in the ubiquitous use of small-size wearable devices around the human body that has unveiled immense possibilities for designing systems that can support applications like music video streaming, social media platforms, online gaming consoles, etc. However, these applications often demand high bandwidth and data rates. The devices in these applications wirelessly interact through traditional radio wave-based communication. Human Body Communication (HBC) has emerged as a promising alternative to traditional wireless communication for energy-efficient information exchange among wearable devices [1], [2]. Among the existing HBC modalities, [3]–[5], capacitive HBC, with its wide bandwidth to support high data throughputs and comparatively lower path loss over long distances, has drawn significant attention.

Previous studies on characterizing the human body channel have been conducted with communicating devices that are not of wearable form factor [6]–[9] and hence the developed understandings may not be applicable while working with wearable devices. The channel characterization for capacitive HBC using miniaturized battery-powered wearables, together with a moderate impedance matching network, was presented over a frequency range from 20 MHz to 150 MHz [10]. Later,

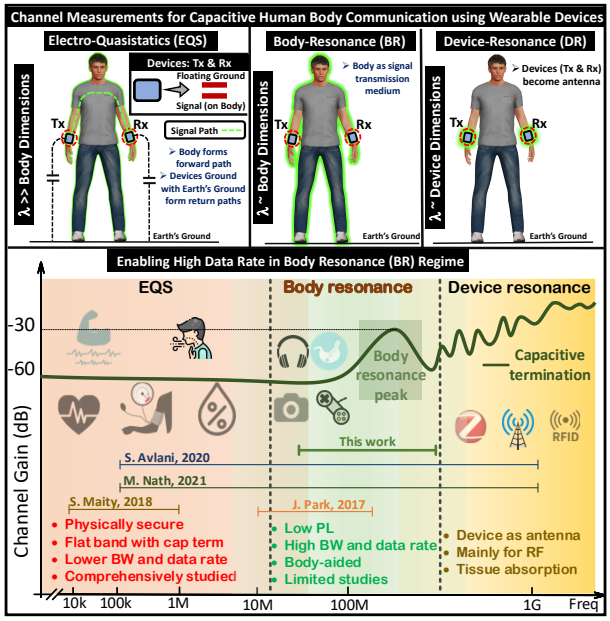

Fig. 1. Schematic representation of the channel characteristic for capacitive Human Body Communication (HBC) over a broad frequency range from a few kHz to tens of GHz. With its lower path loss and high data rate, this paper primarily focuses on channel measurements in the body resonance regime with wearable devices.

channel measurements for capacitive HBC using wearable devices over a broad frequency range (100 kHz to 1 GHz) [11] and the understanding of the three regions, namely EQS, Body Resonance (BR), and Device Resonance, in the channel characteristic has been substantiated through wide-band measurements till 1 GHz [12]. The BR regime refers to a frequency range where the wavelength is of the same order of magnitude as the human body size [12]. Similarly, in the device resonance regime, the frequency is high enough to make the wavelength comparable to the devices. Fig. 1, while portraying the three frequency regimes, summarizes their key attributes.

In the past decade, an extensive exploration of the human body channel characterization for capacitive HBC in the EQS regime [13]–[16], has been carried out. However, owing to the complex nature of the propagating EM wave in, on, and around the human body in the BR regime, the channel variability resulting from the positional variations of the on-body communicating devices in this regime has not been studied through measurements so far. With its higher channel

gain and bandwidth compared to EQS-HBC, the BR regime can be a promising choice for the design of power-efficient HBC systems that require high data rates. This motivates us to explore the human body channel in the BR regime through measurements using carefully designed wearable devices.

II. Simulation Setup and E-Field Comparison

The Finite Element Method (FEM)-based EM simulations are performed using ANSYS High Frequency Structure Simulator (HFSS). A simplified cross-cylindrical human model, shown in Fig. 2(a). made up of skin and muscle tissue [17] whose validity was confirmed [1] through comparison of EM field distribution with a complex human body model - VHP Female v2.2 from Neva Electromagnetics [18] is used to reduce computational time and complexity.

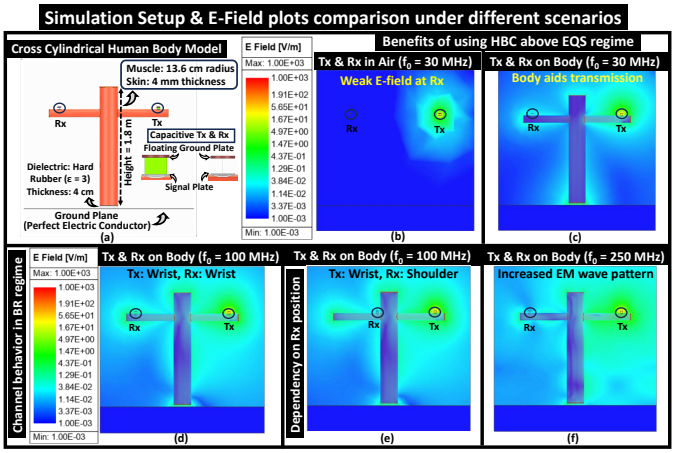

Fig. 2. Simulation Setup: (a) Model used for HFSS simulations and its structural parameters, E-Field Plots comparison: (b) Without Body, (c) With Body, (d) Increased field strength at Rx near BR peak, (e) Dependency on Rx position, (f) Increase in on-body EM wave patterns beyond BR.

Comparison between the E-field distribution under different scenarios, illustrated in Fig. 2 ((b),(c),(d)) highlights the benefits of using HBC in the BR frequency regime and EM patterns formed on the human body which will be explored further through the experimental verifications described in the following section.

III. Experimental Setup

This section delineates the experimental setup used for channel gain measurements. The subject's body posture, the communicating devices (Tx and Rx), and the overall system schematic are shown in Fig. 3. A handheld RF Explorer signal generator (RFE6GEN) is employed as the signal transmitter. With operational frequencies ranging from 24 MHz to 6 GHz and a resolution bandwidth of 1 kHz. The transmitted signal power level is kept at -5 dBm (∼0.5 V peak-to-peak) to keep the in-body field and current densities below the ICNIRP safety limits [19]. A handheld RF Explorer spectrum analyzer (WSUB1G+) with operational frequency ranging from 100 kHz to 960 MHz with a frequency resolution of 1 kHz is used as the wearable receiver. The aluminum-made outer casing of the devices is covered with a thin layer of foam

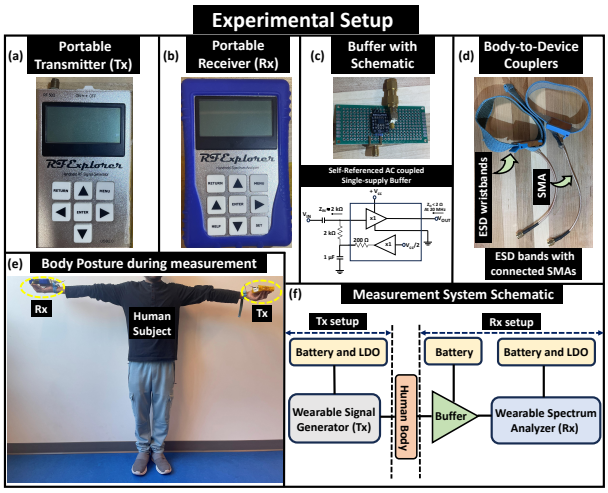

Fig. 3. Experimental Setup: (a) Wearable Transmitter: Portable RF signal generator, (b) Wearable Receiver: Portable RF spectrum analyzer, (c) Buffer and its schematic for high impedance capacitive terminated measurements, (d) Body-to-Device couplers, (e) Body posture: T-pose & Measurement Location: Hall corridor, and (f) Overall system schematic

to avoid any direct contact between the subject's body and the device ground. The Rx, with its 50 Ω input impedance, requires a buffer for high-impedance capacitive termination. A wide bandwidth buffer circuit is made using BUF602, a high-speed buffer IC from Texas Instruments. A small-sized 3.7 V (nominal) rechargeable lipo battery is used to power the setup. Its high bandwidth of 1 GHz and high slew rate of 8000 V/μs make it suitable for handling high-speed AC signals. The high-impedance capacitive termination is ensured by the input impedance of the buffer, which is 1 MΩ in parallel with 2.1 pF. The functionality of the couplers at the Tx and Rx ends is emulated using ESD wristbands, shown in 3.

IV. Experiments and Analysis of Experimental Results

A. Measurement Procedure

The wearable Tx, Rx, and buffer, are calibrated by using a Keysight benchtop signal generator and spectrum analyzer as standard to ensure the accuracy of measurements. The experiments were conducted in a corridor of a hall to minimize undesired couplings and interference from the surroundings and the measurement accuracy was confirmed through its repeatability. The experimental guidelines involving human subjects have been approved by the Institutional Review Board (IRB). The subject with on-body Tx and Rx extends the arms to emulate the T posture. The device-to-device coupling measurement was carried out by keeping Tx and Rx on two wooden stools, separated by a distance that equals the wrist-to-wrist length of the human subject while during subject-to-device coupling measurement, the Tx is worn on one wrist of the subject who extends the arms while the other is placed 15 cm away from the other wrist of the subject. In each experiment, the frequency is swept with an interval of 10 MHz between 30 MHz and 250 MHz. Moreover, Rx

positional sweep measurements were executed by moving it along the arm. These positions are shown in Fig.6.

B. Analysis of Experimental Results

1) On-Body vs Off-Body Communication

The experimental results for the variations in channel characteristics with operational frequency in the BR regime are plotted by averaging multiple measurements of the same scenario while the error bars show the corresponding minimum and maximum values.

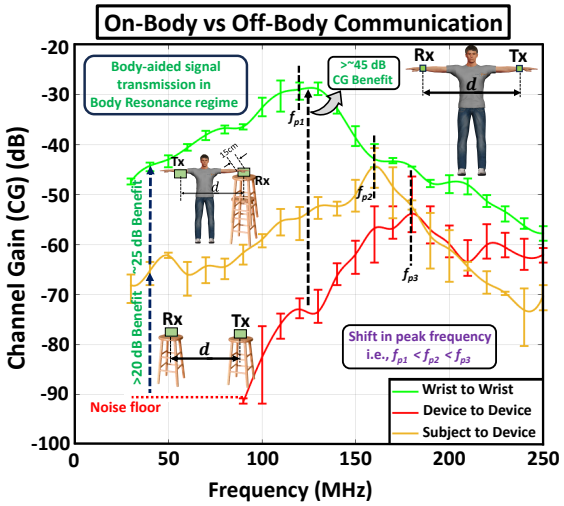

Fig. 4. Channel gain in the body resonance regime under different scenarios: (a) Red Curve: Tx and Rx are communicating through air i.e., Device-to-Device coupling, (b) Yellow curve: Tx is at subject's wrist and the Rx is an off-body device (i.e., 15 cm away from wrist). (c) Green curve: Tx and Rx are on the wrists of opposite arms.

According to Fig. 4, the on-body placement of Tx and Rx offers ∼45 dB improvement in channel gain compared to the device-to-device coupling in air. The human body, with its conducting nature, provides an additional signal path, thereby strengthening the received signal. Moreover, the measurement performed using an on-body Tx and off-body Rx (i.e., 15 cm away from the wrist of the other arm) shows a ∼20 dB improvement in channel gain compared to the in-air device-to-device coupling. According to the results, with the T-posture of the subject, the location of the body-resonance peak remains between 100 to 150 MHz.

2) Frequency Sweeps at Different Receiver Positions

The changes in channel characteristics with frequency for different on-body receiver positions are presented in Fig. 5. It is observed that the Rx movement from the subject's wrist towards the shoulder results in attenuation in channel gain in the BR regime, shown in Fig. 5, an equivalent effect that was perceived and termed as body shadowing in EQS [16].

3) Position Sweeps at Different Operating Frequencies

The channel gain variations with change in on-body Rx position from the wrist of the opposite arm over the chest (i.e., location of largest path loss) and eventually to the same arm

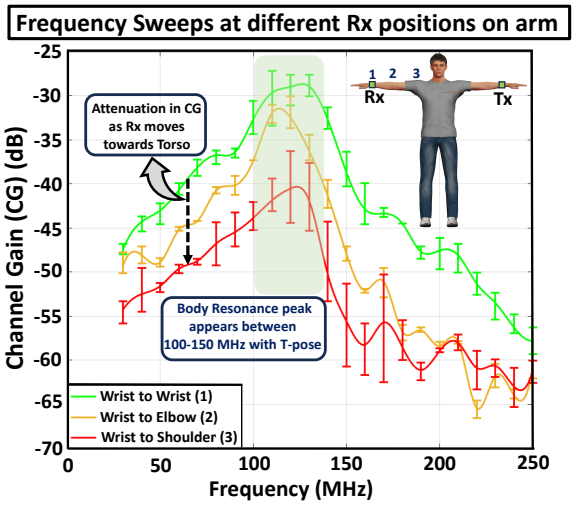

Fig. 5. Channel gain variation at different receiver positions on the subject's arm: While keeping the Tx-position fixed at the subject's wrist when the Rx-position is varied as (a) Rx at the wrist, (b) Rx at the elbow, and (c) Rx at the shoulder.

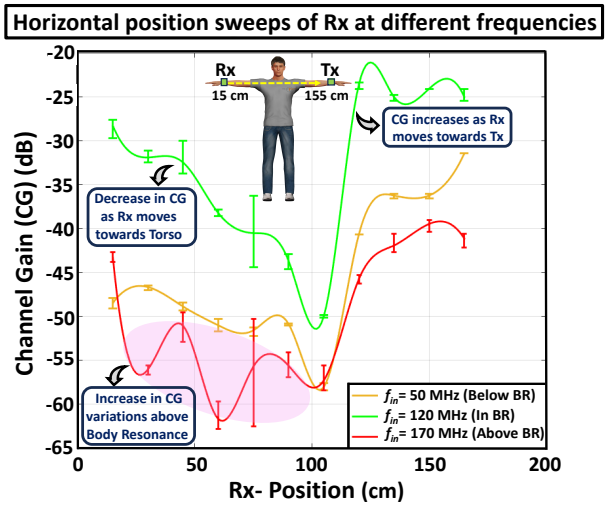

Fig. 6. Effect of change in Rx-position along subject's arm on channel gain at different operating frequencies (f_{op}): (a) f_{op} = 50 MHz (below BR peak), (b) f_{op} = 120 MHz (at BR peak), and (c) f_{op} = 170 MHz (beyond BR peak).

(i.e., location where inter-device coupling starts to dominate) towards the Tx, at three different operating frequencies that lie below BR (50 MHz), around BR (120 MHz), and above BR (170 MHz), are captured in Figs. 6. It can also be observed that an increase in the operating frequency beyond the BR regime (i.e., decrease in wavelength) leads towards the generation of more E-Field patterns on the body, as shown in Fig. 2 (f), and therefore enhances the undulations in the channel gain characteristic.

V. Conclusion

In conclusion, we present the benefits of human body communication in the BR regime and the channel variability from the positional variation of the on-body receiver using carefully designed wearable devices. The results depict that ∼45 dB improvement in channel gain can be achieved via human body communication compared

to over-the-air device-to-device communication. Besides, with the T-posture of the subject, the body resonance peak is observed to appear between 100-150 MHz, and the maximum channel gain at the peak frequency varies with the on-body receiver position. The T-posture for the subject's body is adopted to highlight the feasibility of the proposed technique for long body-centric communication channels in Non-line-of-sight (NLOS) scenarios between the battery-powered communicating devices (Tx & Rx) of wearable form factor. These observations can potentially facilitate building up the theoretical understanding of the body channel feature in the BR regime towards developing power-efficient yet high data rate HBC transceiver systems.

ACKNOWLEDGEMENT

This work was supported by Quasistatics, Inc. under Grant 40003567.

REFERENCES

[1] S. Maity, M. Nath, G. Bhattacharya, B. Chatterjee, and S. Sen, "On the safety of human body communication," *IEEE Transactions on Biomedical Engineering*, vol. 67, no. 12, pp. 3392–3402, 2020.

[2] D. Das, S. Maity, B. Chatterjee, and S. Sen, "Enabling covert body area network using electro-quasistatic human body communication," *Scientific reports*, vol. 9, no. 1, pp. 1–14, 2019.

[3] T. G. Zimmerman, "Personal area networks: Near-field intrabody communication," *IBM systems Journal*, vol. 35, no. 3.4, pp. 609–617, 1996.

[4] M. S. Wegmueller, M. Oberle, N. Felber, N. Kuster, and W. Fichtner, "Signal transmission by galvanic coupling through the human body," *IEEE Transactions on Instrumentation and Measurement*, vol. 59, no. 4, pp. 963–969, 2009.

[5] J. Park and P. P. Mercier, "Magnetic human body communication," in *2015 37th Annual International Conference of the IEEE Engineering in Medicine and Biology Society (EMBC)*. IEEE, 2015, pp. 1841–1844.

[6] B. Tomovski, F. Gräbner, A. Hungsberg, C. Kallmeyer, and M. Linsel, "Effects of electromagnetic field over a human body, sar simulation with and without nanotextile in the frequency range 0.9-1.8 ghz," *Journal of Electrical Engineering*, vol. 62, no. 6, p. 349, 2011.

[7] B. Kibret, A. K. Teshome, and D. Lai, "Analysis of the whole-body averaged specific absorption rate (sar) for far-field exposure of an isolated human body using cylindrical antenna theory," *Progress In Electromagnetics Research M*, vol. 38, pp. 103–112, 2014.

[8] B. Kibret, A. K. Teshome, and D. T. Lai, "Cylindrical antenna theory for the analysis of whole-body averaged specific absorption rate," *IEEE Transactions on Antennas and Propagation*, vol. 63, no. 11, pp. 5224–5229, 2015.

[9] J. Li, Z. Nie, Y. Liu, L. Wang, and Y. Hao, "Evaluation of propagation characteristics using the human body as an antenna," *Sensors*, vol. 17, no. 12, p. 2878, 2017.

[10] J. Park, H. Garudadri, and P. P. Mercier, "Channel modeling of miniaturized battery-powered capacitive human body communication systems," *IEEE Transactions on Biomedical Engineering*, vol. 64, no. 2, pp. 452–462, 2016.

[11] S. Avlani, M. Nath, S. Maity, and S. Sen, "A 100khz-1ghz termination-dependent human body communication channel measurement using miniaturized wearable devices," in *2020 Design, Automation & Test in Europe Conference & Exhibition (DATE)*. IEEE, 2020, pp. 650–653.

[12] M. Nath, S. Maity, S. Avlani, S. Weigand, and S. Sen, "Inter-body coupling in electro-quasistatic human body communication: Theory and analysis of security and interference properties," *Scientific Reports*, vol. 11, no. 1, pp. 1–15, 2021.

[13] S. Maity, D. Das, and S. Sen, "Wearable health monitoring using capacitive voltage-mode human body communication," in *2017 39th Annual International Conference of the IEEE Engineering in Medicine and Biology Society (EMBC)*. IEEE, 2017, pp. 1–4.

[14] S. Maity, M. He, M. Nath, D. Das, B. Chatterjee, and S. Sen, "Bio-physical modeling, characterization, and optimization of electro-quasistatic human body communication," *IEEE Transactions on Biomedical Engineering*, vol. 66, no. 6, pp. 1791–1802, 2018.

[15] M. Nath, S. Maity, and S. Sen, "Toward understanding the return path capacitance in capacitive human body communication," *IEEE Transactions on Circuits and Systems II: Express Briefs*, vol. 67, no. 10, pp. 1879–1883, 2019.

[16] A. Datta, M. Nath, D. Yang, and S. Sen, "Advanced biophysical model to capture channel variability for eqs capacitive hbc," *IEEE Transactions on Biomedical Engineering*, 2021.

[17] S. Gabriel et al., "The dielectric properties of biological tissues: II. measurements in the frequency range 10 hz to 20 GHz," *Physics in Medicine and Biology*, vol. 41, no. 11, pp. 2251–2269, nov 1996.

[18] "NEVA Electromagnetics LLC | VHP-Female model v2.2 - VHP-Female College," https://www.nevaelectromagnetics.com/vhp-female-2-2, [accessed August 27, 2020].

[19] ICNIRP, "ICNIRP guidelines for limiting exposure to electromagnetic fields (100 kHZ to 300 GHZ)," *Health Phys.*, vol. 74, no. 4, pp. 483–524, 2020.